

Novel separation process for obtaining recycled cement and high-quality recycled sand from waste hardened concrete

Ana Carriço^a, José Alexandre Bogas^{a,*}, Susana Hu^a, Sofia Real^a,
Manuel Francisco Costa Pereira^b

^a CERIS, Instituto Superior Técnico, Universidade de Lisboa, Av. Rovisco Pais, 1049-001, Lisbon, Portugal

^b CERENA, Instituto Superior Técnico, Universidade de Lisboa, Av. Rovisco Pais, 1049-001, Lisbon, Portugal

ARTICLE INFO

Handling editor: Zhen Leng

Keywords:

Recycled cement
Cleaner recycled aggregate
Concrete separation
Magnetic separation
Thermal activation

ABSTRACT

Separation is a fundamental step for concrete recycling, enabling not only the achievement of reliable and cleaner recycled aggregates but also the better re-use of the remaining concrete constituents. Recently, a new hydraulic binder produced from the hydrated cement paste contained in waste concrete, which is associated with lower processing temperatures and carbon dioxide emissions, has gained momentum in the history of concrete recycling. However, a decisive turning point for its application lies in the successful individualisation of the cement paste and aggregate initially contained in concrete debris. This paper describes a new patented method involving a mechanical comminution stage and a high-intensity magnetic separation process to obtain the cementitious fraction in concrete and retrieve cleaner fine aggregate. The efficiency of the proposed method was assessed through image analysis, thermogravimetry, X-ray diffraction and acid attack. In addition, cement pastes produced with the obtained recycled cement after thermal activation were characterised in terms of mechanical strength. Findings suggest that the proposed method effectively separated the main concrete constituents, especially when the waste material was reduced to the size range 150–500 µm. It was possible to obtain a recycled binder at the current laboratory scale with up to about 80% cement content by weight (nearly 90% in volume). Furthermore, a cleaner recycled fine aggregate, with minimal cement paste contamination, as low as less than 3 wt%, was also obtained. The mechanical strength of pastes with recycled cement retrieved from waste concrete was about 70% of that of reference pastes of equal water/binder produced with recycled cement from non-contaminated waste cement pastes.

1. Introduction

In its many production stages, concrete is a carbon intensive product, with over 80% of emissions residing in its hydraulic binder (Letelier et al., 2017). Furthermore, due to the substantial implementation of concrete in the construction industry, the growth of building stock at end-of-life has also risen. The latest Eurostat data (Eurostat, 2020) reports that, in Europe alone, at least 450 to 500 million tons of construction and demolition waste (CDW) is generated annually, of which one to two-thirds is concrete waste (Shi et al., 2016). The Waste Framework Directive 2008/98/EC, amended by directive 2018/851 (European Union, 2018) targeted that by 2020, 70% of generated CDW must be “prepared for re-use, recycled or undergo other material recovery”. Currently, many EU countries are only able to fulfil this

criterion with backfilling operations, which fall under a low-grade material recovery category (Deloitte, 2017; European Union, 2011).

Recycling concrete waste with the aim of producing recycled aggregate concrete has been extensively investigated and reviewed (Chen et al., 2019), but its wide application in the construction market still faces some challenges (Silva et al., 2017). This is because current methods of processing concrete debris for its use as recycled aggregates have not been efficient in removing the adhered cement paste (Mistri et al., 2020). Although it depends on the characteristics of the original concrete, the adhered paste is the lead contributing factor for the increase of water absorption in the aggregates, with repercussions on fresh concrete properties, as well as in increasing the delayed volume change and in reducing the mechanical strength and durability of concrete (Shi et al., 2016). Similar problems are reported when sand is replaced by

* Corresponding author.

E-mail addresses: ana.carriço@tecnico.ulisboa.pt (A. Carriço), jose.bogas@tecnico.ulisboa.pt (J.A. Bogas), susana.hu@tecnico.ulisboa.pt (S. Hu), sofia.real@tecnico.ulisboa.pt (S. Real), mfc@tecnico.ulisboa.pt (M.F. Costa Pereira).

<https://doi.org/10.1016/j.jclepro.2021.127375>

Received 5 March 2021; Received in revised form 20 April 2021; Accepted 30 April 2021

Available online 8 May 2021

0959-6526/© 2021 Elsevier Ltd. All rights reserved.

fine recycled aggregates (Tahar et al., 2016). Sand represents a substantial fraction of concrete mixtures (approx. 25–35%), further contributing to the increasing scarcity of this natural resource (UNEP, 2019). In Europe, over 1 billion tonnes of sand are produced, being about 1/3 of the total amount of aggregate consumption (UEPG, 2020). Consequently, alternatives to natural sand in concrete have also been the focus of recent research (Kirthika et al., 2020). However, although the use of recycled aggregates contributes to reducing landfill waste and consumption of natural resources, it is still far from solving the problem of high CO₂ emissions of concrete, which is essentially attributed to clinker production.

Therefore, the current main priority of the construction industry is to seek alternative solutions that will lead to economically efficient and sustainable cements. In this context, the production of recycled cement (RC), obtained from concrete waste, has been proposed and recently investigated by various authors (Bogas et al., 2019; He et al., 2019; Wang et al., 2018). Basically, RC is obtained by thermal activation of waste cementitious materials at temperatures much lower than those currently practiced by the cement industry. During the thermal treatment, waste cement undergoes a heating procedure, usually performed between 600 and 700 °C, where dehydration of cement's hydrated phases occurs, thus recovering the hydraulic binding properties of cement (Carriço et al., 2020). Results have shown the potentiality of RC to attain mechanical strength comparable to that obtained by other hydraulic binders while being submitted to a lower processing temperature (Bogas et al., 2019) and involving low levels of CO₂ emission (He et al., 2019). However, one of the main obstacles that has hindered the production of this cement on an industrial scale is related to the difficulties inherent to the processing of concrete debris, namely the individualisation of the cement matrix from the remaining concrete constituents (Bogas et al., 2019; Wang et al., 2018).

Efforts have been made to develop separation processes for concrete waste, essentially aiming to obtain recycled aggregates of better quality. These processes generally use one or combined methods that can be grouped in mechanical, thermal, chemical or gravity separation techniques (Akbarnezhad and Ong, 2013). Mechanical separation techniques involve different methodologies resorting to crushing, impact, grinding and abrasion stages. Some authors suggest that crushing rather than impact achieves lower rates of broken aggregate particles (Hansen, 1992; Lotfi et al., 2014), while grinding autogenously or in ball mills promotes wear and consequent removal of the adhered mortar (Al-Bayati et al., 2016). The efficiency of these methods is conditioned by the mortar strength and aggregate type. For softer aggregates (limestone), fine fractions can be significantly contaminated due to breaking and powdering (Akbarnezhad and Ong, 2013).

In thermal separation techniques, concrete waste is previously heated to temperatures around 300 to 600 °C (Mulder et al., 2007; Sui and Mueller, 2012). After cooling, the material is usually subjected to mechanical action and sieving. This method takes advantage of the different thermal expansion coefficients and mechanical properties of cement paste and aggregates, being less efficient for common limestone concretes (Akbarnezhad and Ong, 2013). Moreover, the thermal process involves high energy consumption, long processing times and partial changes in the physical and mechanical characteristics of separated constituents (Al-Bayati et al., 2016; Nirry et al., 2013).

Gravity separation using specific density liquids allows a direct separation of the constituents but is not environmentally friendly and is associated with high costs and additional steps of decontamination and cleaning of the separated material. Chemical methods have also been considered, usually considering the acid attack of adhered paste (Tam et al., 2007). However, they do not allow the re-use of the cementitious material and are not viable for limestone concretes. Recently, other innovative methods have been suggested, such as microwave (Bru et al., 2014), ultrasound (Katz, 2004), or electric pulse power (Shigeishi, 2017) techniques, but involve high energy consumption and are challenging to implement industrially.

In short, despite various research efforts, there is still no truly attractive methodology for the effective separation of aggregates and cement paste, especially with low economic and environmental impact. The various processes referred to are mainly methodologies that aim at releasing the various constituents from one another, then proceeded by simple sieving as the final step, aided or not with air classifiers, which generally results in high levels of contamination.

The novel procedure proposed in this paper, which is protected under patent (Bogas et al., 2020b), is based on the separation of concrete constituents with high-intensity permanent magnets, benefiting from their distinct magnetic properties. The most common minerals in the aggregates are quartz, feldspar and calcite, which have diamagnetic properties, i.e., their electrons are grouped in pairs with anti-parallel spins, leading to approximately zero magnetic moments with negative magnetic susceptibility (Rosenblum and Brownfield, 2000). The mass magnetic susceptibility of quartz and calcite are reported to be -6.0×10^{-9} and -4.8×10^{-9} m³/kg, respectively (Svoboda, 2004). This low negative magnetic susceptibility promotes a slight repulsion of the aggregate particles in the opposite direction to a high-intensity magnetic field. Contrarily, cement has paramagnetic characteristics, i.e., the electronic structure has unpaired and unparallel spins (Svoboda, 2004). Gopalakrishnan et al. (2012) report a mass susceptibility for anhydrous Portland cement of about 11.4×10^{-7} m³/kg. This positive susceptibility results from the iron oxides present in the ferrous phases of cement and their hydration products. However, due to its low susceptibility, only high intensity and high gradient separators are suitable for cement separation. This is the example of dry magnetic separation with permanent rollers made from rare earth magnets, such as neodymium-iron-boron (NdFeB), which are considered in this study. Permanent magnets have the advantage of easy installation (simple support facilities), good productivity, stable magnetic field, low operating costs and no requirement of a power source or cooling systems (Svoboda, 2004). Compared to other mentioned methods, the high-intensity magnetic separation is a cleaner and less energy-intensive method, with lower economic and environmental impact. One drawback of this method is that the field intensity can not be changed or switched off.

Thus, this study presents and evaluates a new methodology, which aims to fine-tune the final stage of separation, allowing the recovery of more purified cement waste for RCC production and achieving high-quality cleaner fine recycled aggregates. The new suggested method aims to be a step forward towards the ambitious objective of producing fully recycled concrete.

2. Experimental program

An extensive experimental campaign was carried out in order to implement the proposed method of waste concrete separation and evaluate its efficiency. To this end, lab produced well-hydrated waste concrete of known composition was subjected to the proposed separation method and its efficiency was accessed through image analysis, thermogravimetry, X-ray diffraction and acid attack. In addition, cement pastes produced with recycled cement thermoactivated from the separated high-purity cement fraction were characterised in terms of mechanical strength. This section initially presents the new method proposed for the separation of hardened concrete constituents and then the tests used to assess concrete separation quality.

2.1. Proposed procedure for the separation of hardened concrete constituents

The proposed method for separating concrete constituents essentially involves two phases; the concrete comminution with the detachment of hydrated cement paste (liberation) and the individualisation of concrete constituents through a magnetic separation process (separation). The previous phase of concrete comminution is essential to release

the distinct concrete phases from each other and obtain fine particles in a narrow range, necessary for the effective magnetic separation.

Initially, differently sized jaw crushers combined with a roller press, autogenous grinding and grinding with steel balls were tested, and their efficiency in liberating the cementitious phase was compared through image analysis. The highest liberation degree was attained for fractions below 1 mm, which also contained the highest amount of cement paste. However, the magnetic separation underperforms for particles smaller than 125/150 μm . Below this size range, the particles are strongly influenced by secondary effects, such as the adhesion to other particles and the conveyor belt and trajectory changes due to air convection. Therefore, the comminution processes were designed to maximise the fractions between 125 and 1000 μm , involving jaw crushers and a roller mill, which were complemented with intermediate sieving. The autogenous and ball milling were disregarded because they are high-energy consuming and produce a large volume of fines under 125 μm .

A flowchart with the adopted liberation process is presented in Appendices (Figure A1). In a first stage, an oversize jaw crusher, simulating the crushing process of industrial CDW treatment, was used to reduce the waste concrete blocks into particles of up to 30 mm. Then, the material lower than 1 mm was separated by sieving and the upper fraction was further crushed in a small jaw crusher into particles smaller than 12 mm. Afterwards, particles above 1 mm were subjected to two rounds through a roller press, interspersed with sieving through the 1 mm mesh. The material retained in the 1 mm sieve was not significant (<2%). Finally, particles below 1 mm were separated into the following granulometric fractions; <125 μm ; 125–250 μm ; 250–500 μm and 500 μm –1 mm.

The magnetic separation procedure was carried out on the three subdivided size fractions over 125 μm . Since magnetic separation is affected by the presence of very fine particles and dust, which inevitably result from the previous comminution processes, the material was washed through wet screening and dried at 80 °C before being scanned in the high-intensity magnetic roller.

The equipment used had a magnetic roll with 1 T of magnetic field intensity on its surface, with a diameter of 76 mm, and a conveyor belt 1.5 mm thick and 100 mm wide, moving at approximately 40 m/min. At the roller base, an adjustable divider separates the magnetic from the non-magnetic material (Fig. 1). This divider was adjusted based on the trajectory of the feed's particles, which depends on the granulometry, feeding speed and magnetic susceptibility of the material. A monolayer feeding was guaranteed for the various particles to be equally affected by the roller's magnetic force.

Since concrete is mostly composed of aggregates (non-magnetic material), an inverse methodology for the separation was chosen. The first scan aims to eliminate most non-magnetic material (NM), with a wide opening in the divider and faster feeding speed, corresponding to high-quality sand with low adhered mortar. Then, in subsequent scans, the material retained as magnetic was successively purified in the magnetic roller with a narrower opening and slower feeding speed. Thus, only particles with the closest trajectory to the magnetic field are

recovered in order to obtain a magnetic material of higher purity. From three scans, the magnetic products of increasing purity, M1→M2→M3, were obtained.

The suggested magnetic method has the advantage of being a green procedure with minimal energy consumption and with low environmental impact (without chemicals and thermal treatments, neglecting emissions and low levels of noise and powder generation). The major drawback is the washing and drying stage before the magnetic separation, which can be avoided if more powerful high-intensity magnets are considered. Existing permanent industrial rollers of higher diameter and higher field intensity, near 2 T, are expected to be more effective in waste concrete separation.

2.2. Waste concrete production

Source concrete (SC) was produced with 670 L/m³ of aggregate with an average density of 2640 kg/m³ and 360 kg/m³ of CEM I 42.5 R with a particle density of 3070 kg/m³, for a water to cement ratio (w/c) of 0.55. The aggregate fraction was composed of three types of crushed limestone aggregates of different granulometric sizes and coarse and fine natural siliceous sand. The average compressive strength of SC at 28 days was 46.2 MPa.

Source cement paste (SP) was also prepared for comparison purposes, with the same w/c ratio as SC. The average 28 days compressive strength was 41.1 MPa. SC was moulded in 300x150 × 150 mm³ prismatic specimens, and SP was moulded in $\phi 150 \times 300$ mm cylindrical specimens. After 24 h, specimens were demoulded, watered periodically for 7 days and then air cured for at least 3 months. The hydration degree of SP, determined from thermogravimetric analysis, was near 80%, representative of a well-hydrated cement paste.

2.3. Image analysis

Visual analysis of the samples provided the first assessment of the degree of liberation achieved by the comminution methods and of the efficiency of the magnetic separation. The image analysis was performed using a digital microscope model AM7915 MZt from Dino-Lite, with 5 MP resolution and up to 220x magnification. Samples were randomly collected from each size fraction, using the quartering sample division, and analysed under the same magnification and contrast conditions. The equipment enables sharp observation of particles with a minimum size of 100 μm , losing focus for smaller particles. Moreover, below 100 μm , the distinction between hydrated calcium silicate phases and the aggregate fraction becomes less clear due to their identical colour tone.

2.4. Thermogravimetric analysis

Thermogravimetric (TG) analysis was performed to evaluate the amount of cement in each size fraction obtained by the comminution of source concrete, as well as in the respective magnetic and non-magnetic products. Due to the large number of samples, expedite discontinuous

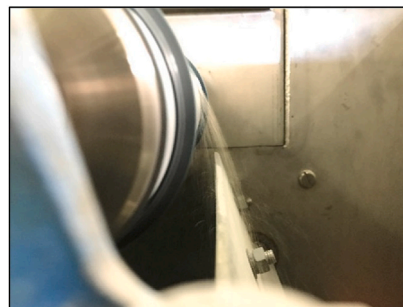
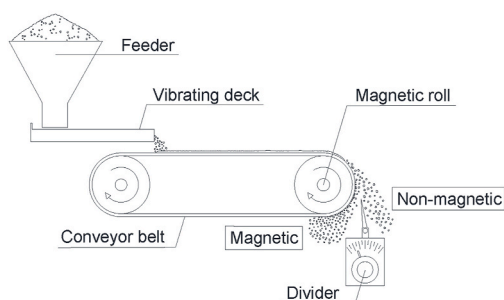


Fig. 1. Schematic representation of the high-intensity magnetic separation process considered in this study (left) with effective separation of paramagnetic cement particles (right).

TG analyses were performed in a muffle, herein designated as partial TG (PTG). This method allowed the estimation of the cement content in each sample by measuring, at specific temperatures, the discrete weight change due to loss of combined water in the hydrated compounds.

The PTG was initially calibrated from preliminary TG analysis in order to define an adequate operating temperature range. Carbonation due to handling and storage can influence the mass variation and the onset temperature of the main reactions. Moreover, mass loss due to portlandite dehydroxylation, usually in the 400–600 °C temperature range (Collier, 2016), can be offset to the decarbonation region (>600 °C), due to portlandite carbonation. This would lead to imprecise estimations of the cement content. However, the mass loss of cement paste in the 150–350 °C range is not significantly affected by previous carbonation, and the mass loss of aggregates is negligible in this region. Therefore, this temperature range was set to estimate the cement content.

Each sample was ground to a fine powder (<125 µm), pre-conditioned at 150 °C for 12 h to remove free water and cooled to room temperature in a desiccator to avoid ambient moisture uptake. Then, two samples of about 10 g each were placed in a crucible and heated in a muffle furnace at a rate of 10 °C/min until 350 °C, with a residence time at this temperature of 2 h. The samples were cooled in the muffle to 150 °C and in a desiccator until ambient temperature. The mass loss for the 150–350 °C range of reference samples with only cement paste (L_P) and only the aggregate fraction (L_A) were also determined. This allows the estimate of the cement paste content in each sample according to Equation (1) (by weight, wt%). Despite the negligible mass loss of aggregates, the mass loss of each sample (L_M) was corrected by the L_A (of 0.15 wt%, on average).

$$\% \text{ cement paste} = \frac{L_M - L_A}{L_P - L_A} \quad (1)$$

To validate the expedite PTG method, pre-mixed reference samples with known amount of sand and waste SP were prepared and subjected to the procedure described above. The cement contents obtained in the reference mixes with 10, 25, 50, 75 and 90 wt% waste cement were 10.6, 25.8, 51.5, 75 and 87.1 wt%, respectively. Overall, the maximum error of the cement content estimated by PTG was below 6 wt%.

In addition, the method was further validated by conventional continuous TG analysis conducted for one sample of the 250–500 µm magnetic fraction and the reference cement paste (SP) (Fig. 2). A SETARAM thermobalance, model TGA92, was used with N₂ atmosphere and a heating rate of 10 °C/min. Comparing the mass loss in both samples between 150 and 350 °C, the estimated cement paste content in the 250–500 µm fraction was 78 wt%. This value was very near the 79 wt % estimated from PTG, for the same temperature range, which supports the validity of the method adopted in this study.

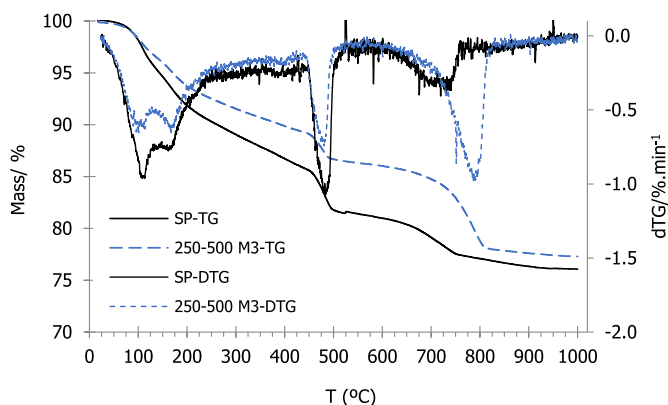


Fig. 2. Thermogravimetric analysis: TG curves and first derivative (DTG) of SP and M3 of size fraction 250–500 µm.

2.5. Acid attack

A hydrochloric acid solution was used to determine the siliceous sand content in the mixtures. The acid attacks clinker minerals by dissolving calcium ions in the solution, which is subsequently leached out by decantation. Besides portlandite and other calcium bearing hydration products in cement paste, limestone aggregates are also attacked, leaving sand as the only remaining fraction. Two samples of each product per size fraction were tested. The procedure consisted of mixing 1 g of the oven-dried mixture with 50 mL of distilled water and 3 mL of hydrochloric acid (about 33% concentration). The mixture is mixed in a magnetic stirrer for a few minutes and then progressively decanted to a pH over 6. Finally, the remaining material is oven-dried and its weight is compared to that of the initial sample.

2.6. X-ray diffraction (XRD)

XRD was performed for phase identification and to analyse the relative phase proportion within each sample. One sample of about 5g was tested per product. A PANalytical X'Pert Pro diffractometer with an angular variation of 2θ, between 5 and 70 °C, a step size of 0.03° and a time step of 75 s was used. Cu radiation was generated using 35 mA and 45 kV operating conditions.

2.7. Mozley table

The Mozley table was employed to assess the maximum liberation degree attained in each size fraction. This is an efficient gravitational separation method that distinguishes materials with similar density. The table has a V-shaped design, where the heavier materials (aggregates) accumulate at the bottom while the lighter particles (cement paste) rise to the water surface. Particles are then forwarded by a water flow to the opposite end of the table, while oscillatory movements promote material separation. The lighter cement paste particles are forwarded first and collected. This material corresponds to individualised cement paste particles that were successfully liberated or had minimal aggregate content. The purity of this fraction is then accessed by PTG. This separation relies on visual observation to cut between both phases. Moreover, the method is discontinuous, not allowing a continuous feeding of the material. Therefore, its use is limited to the analysis of the maximum achievable liberation in each size fraction. A 100 g sample was used for each fraction, and the table slope, water flow, and oscillatory velocity were adjusted accordingly.

2.8. Production and mechanical characterisation of recycled cement paste

The novel method described in this study was designed to recover the cementitious fraction from waste concrete to produce thermoactivated recycled cement (Figure A1 in Appendices). In this case, the purest magnetic fraction (M3), with the highest cement content (determined by PTG), was selected to produce the thermoactivated recycled cement.

After magnetic separation, the cement fraction was ground in a Denver ball mill until all the material passed the 125 µm sieve. Thermal activation was performed in a horizontal oven with a heating rate of 15 °C/min up to a maximum temperature of 700 °C, remaining at this temperature for 3 h. The thermal treatment was defined according to previous works of the authors (Bogas et al., 2019; Carriço et al., 2020b). Then, the thermoactivated material was cooled inside the oven to room temperature. Two sets of pastes were produced with recycled cement from the purest magnetic fraction (M3RC) and with reference recycled cement (RRC), directly obtained from source paste, with the same w/c of source concrete. The RRC paste was produced with normal consistency according to EN 196–3 (CEN, 2016), which corresponded to w/c of 0.71. The M3RC paste was produced with the same w/c for comparison purposes. The high w/c of these pastes is attributed to the great water demand of the recycled cement with high surface area (Carriço et al.,

2020a; Real et al., 2020).

Nine prisms with $40 \times 40 \times 160 \text{ mm}^3$, per each composition, were cast to be tested for flexural and compressive strength at 3, 7 and 28 days. After 24 h, the specimens were demoulded and cured in a wet chamber with relative humidity over 95% until testing age. The tests were performed in a Seidner Form + Test HD-7950 Riedlingen, according to EN 1015-11 (CEN, 2019).

3. Results and discussion

3.1. Yield from liberation and magnetic separation methods

Figure A2 in Appendices presents an overview of the material yield in each of the method's main processes described in this study. The liberation phase's yield was measured by the final mass percentage of each size fraction to the waste concrete blocks' initial mass. The adopted procedure effectively reduced the number of particles over or under the targeted size range (between $125 \mu\text{m}$ and 1 mm). As mentioned, only less than 2% was retained in the 1 mm sieve and about 10% passed the $125 \mu\text{m}$ sieve. Therefore, the pre-classified size fractions, suitable for magnetic separation, retained approx. 90 wt% of the initial material, which was essential in assuring the maximum volume of particles proceeded to magnetic separation. An additional round in the roller press could have been undertaken to reduce the amount of material over 1 mm . However, balancing the amount of lost material and the extra time and energy consumption deemed this complementary step unnecessary. Nevertheless, a high cement paste content can be lost in the finer particles ($<125 \mu\text{m}$) that are not subjected to the magnetic separation. This issue will be addressed further in section 3.3, as well as the efficient release of the cement matrix from aggregates (liberation) attained in each fraction size.

Fig. 3 presents the material yield from the magnetic process, which corresponds to the percentage of magnetic and non-magnetic products to the initial material mass of each size fraction. The magnetic fractions are divided into three different products of increased purity M1, M2 and M3. The cement yield represented in Figure A2 in Appendices pertains to the effective cement content that can be retrieved by the novel method and will be addressed in section 3.3.

The magnetic fraction (M2) yield varied significantly (5–25 wt%) with the size fraction (Fig. 3). In this case, various factors, such as the cement content, particle weight, dust content and the liberation degree attained by mechanical comminution, play an essential role in the amount of cementitious material that can be recovered through magnetic separation. The percentage of the most magnetic materials (M2, M3) increased with the reduction of the particle size fraction: 24.0, 16.5 and 5.5 wt% for the range $125\text{--}250 \mu\text{m}$, $250\text{--}500 \mu\text{m}$ and $500\text{--}1000 \mu\text{m}$,

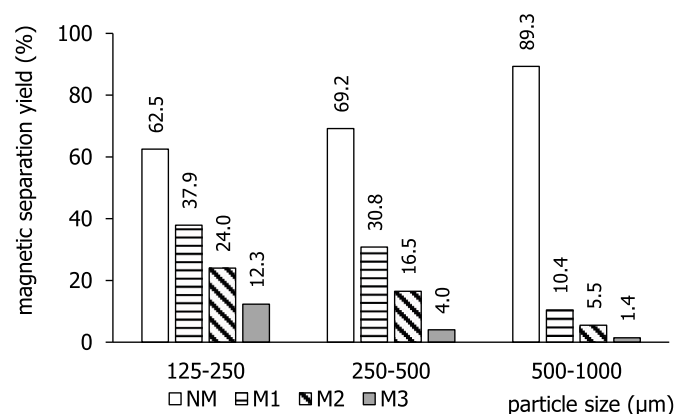


Fig. 3. Weight percentage of waste material yield for each size fraction after magnetic separation: non-magnetic material from a 1st scan (NM), the magnetic product of the 1st scan (M1), 2nd scan (M2) and 3rd scan (M3).

respectively. This is related to the higher cement content and liberation degree attained in the finer fractions, as discussed in 3.3. This study's relative low separation yield can be improved at an industrial scale by using a larger and more powerful roller that may provide higher magnetic field intensity and extended contact area between particles and the magnetic field (higher roller diameter).

3.2. Qualitative image analysis

The liberation degree was first accessed by image analysis. Particles obtained from the comminution methods may be classified according to the scheme presented in Fig. 4. In Fig. 5, the mixtures obtained by the comminution processes were divided into the three granulometric fractions that were the focus of this study. The aggregates, composed of limestone and siliceous sand particles, showed a range of clear to yellowish and orange tones that contrast against the grey cement paste particles. Additionally, limestone aggregates tend to have sharper edges due to the comminution processes, while sand particles exhibit smoother surfaces with a polished texture. As expected, a visual observation confirmed that aggregate/cement paste liberation increased with decreasing particle size. Furthermore, for same-sized fractions, cement paste particles tend to be finer than aggregate particles, which may be related to their lower hardness and higher susceptibility to fragmentation.

Overall, the magnetic method separated the aggregate and cement particles adequately (Fig. 5). The $125\text{--}250 \mu\text{m}$ size fraction showed liberated type e) aggregate particles in the magnetically separated fraction, which indicates that some contamination of the magnetic fraction occurred (Fig. 5g)). In fact, the lighter and finer particles are subjected to the enhanced action of secondary effects, such as air drafts, which can disrupt the particle's trajectory. Additionally, the smaller the particle size, the harder it is to guarantee a monolayer of material over the conveyor belt, an essential condition for the effective separation of the particles. These side-effects may be minimised with larger rollers of higher field intensity and increasing the number of scans.

Particles between 250 and $500 \mu\text{m}$ showed the lowest contamination degree in either fraction (Fig. 5e,h)), with many type a) and e) particles in the initial mix. Although few type d) cement particles can still be found in the non-magnetic fractions, preliminary visual observation showed that a relatively uncontaminated aggregate and cement phase were successfully obtained through magnetic separation in this size fraction. On the other hand, coarser particles in the upper range ($500\text{--}1000 \mu\text{m}$) showed a significantly higher contamination level in magnetic and non-magnetic fractions than in the range $125\text{--}500 \mu\text{m}$. However, according to Fig. 5c) this is probably due to the poor liberation achieved by previous comminution methods. Various particles were

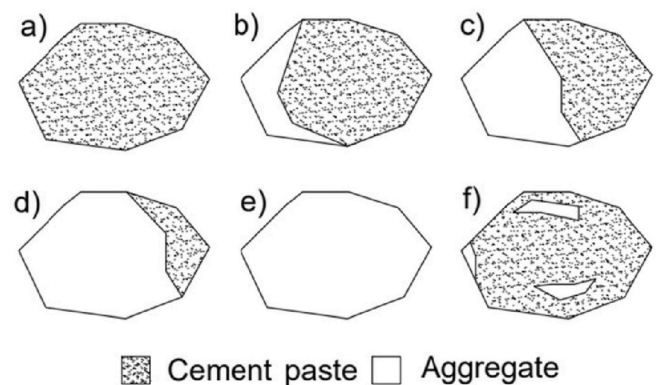


Fig. 4. Types of particle obtained by the comminution processes (indicative percentages): a) $> 90\%$ cement; b) $60\text{--}90\%$ cement; c) $40\text{--}60\%$ cement; d) $10\text{--}40\%$ cement; e) $< 10\%$ cement and f) aggregate covered by cement ($<20\%$ cement).

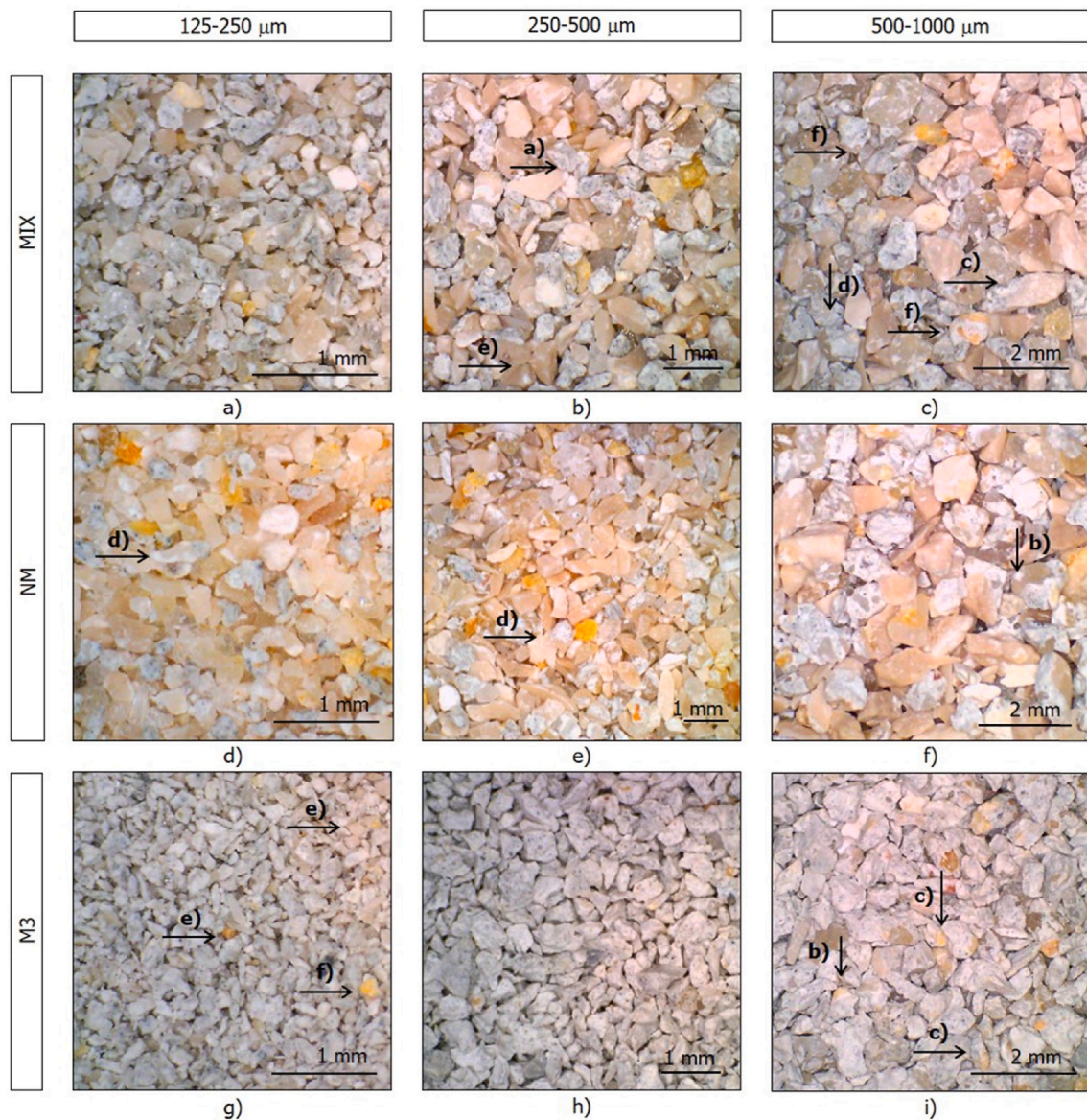


Fig. 5. Mixture (MIX), non-magnetic (NM) and magnetic (M3) materials for each size fraction.

identified with a blended composition of aggregate and cement paste (type c), d) and f) particles), indicating that they did not break through the paste-aggregate interface, which led to apparent contamination of the magnetic and non-magnetic fractions.

3.3. Estimation of cement content from TG analysis

The cement content was determined from samples obtained after the initial comminution methods and after the three magnetic separation scans that followed. Fig. 6 presents the cement content of these samples in each size fraction, which was determined based on the mass loss between 150 and 350 °C, according to Equation (1), in section 2.4. The error between two samples for the cement content by TG was lower than 5%.

The cement content of the initial mixture (MIX) increased with the reduction of the fraction size (Fig. 6), from the 500–1000 μm towards the 125–250 μm range. In fact, the comminution process tends to accumulate more cement in the finer fractions, as has also been reported by other authors (Angulo et al., 2009; Krouer et al., 2020).

On average, for the 250–500 μm size fraction, after magnetic

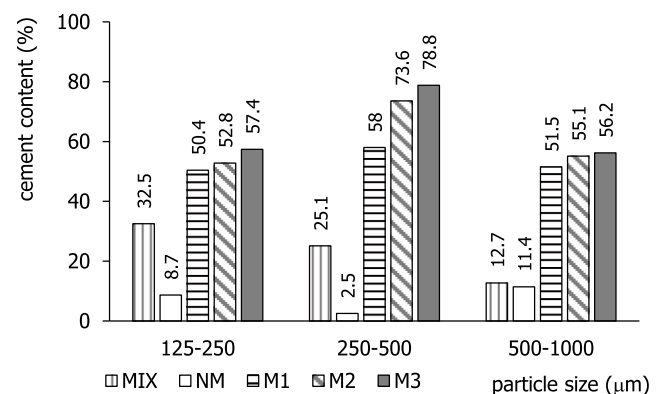


Fig. 6. Cement content of the different materials: initial mixture (MIX), non-magnetic material obtained from the first scan (NM) and magnetic products (M1, M2, M3).

separation, the cement content increased from 25 wt% in the original mixture (MIX) to nearly 80 wt% in the magnetic fractions (M3). The cement content increased significantly after the first two scans of the material through the magnetic field. However, a third scan had no relevant benefit, as the final products (M2, M3) showed similar cement content.

Particles in the 500–1000 μm range yielded a considerably lower cement content, below 60 wt%. In this case, as found in section 3.2, the inefficiency is not directly related to the magnetic separation procedure but to the insufficient aggregate/cement liberation that was achieved in the comminution processes. This is evidenced by the negligible difference between the average cement content of M2 and M3 in this size fraction.

The mixture that initially contained the greatest amount of cement paste (32.5 wt%), with particle size between 125 and 250 μm , retrieved a cement content of up to only 60 wt%, which was lower than what would be expected based on the liberation level found in the image analysis performed in section 3.2. This issue was explored further by subdividing the initial mix into narrower fractions: 125–150 μm ; 150–212 μm and 212–250 μm . Fig. 7 shows the magnetic material obtained after one scan in each size fraction and the respective cement paste and aggregate content.

On the one hand, magnetic separation performs better with narrow-sized fractions, where all particles present similar sizes. On the other hand, coarser particles within the 125–250 μm range, namely over 150 μm , are less subjected to the adverse adhesion effects mentioned in section 2.1. The upper sized fractions (>150 μm) contained on average 75 wt% cement paste, which is closer to that obtained in the 250–500 μm particle range. Based on these results, magnetic separation showed limited efficiency for fractions with particle size lower than 150 μm , and more satisfactory results were obtained for granulometric size fractions between 150 and 500 μm . Thus, it is concluded that this method should be applied for particle sizes over 150 μm , at least for the roller size and field intensity considered in this study. On average, the amount of waste material between 125 and 150 μm represented around 39% of the fraction 125–250 μm .

It is important to note that the non-magnetic material collected in the

first scan contained a reduced amount of cement paste (Fig. 6), especially in the 250–500 μm range (<3 wt%). This confirms that, for all size fractions, high-quality recycled sand with low adhered cement paste may be obtained using the procedure described in this study, as illustrated in Fig. 5d) and e),f). The non-magnetic fraction with higher cement content (~11 wt%) occurred in the 500–1000 μm size fraction, supporting that this range exhibited the lowest degree of liberation between aggregate and cement paste. Moreover, the cement content in the aggregate fraction was only slightly lower than that of the original mixture (Fig. 6), which also signals a less effective liberation and separation of concrete constituents in this fraction.

Globally, and referring to Figure A2 in Appendices, in the least contaminated size fraction (250–500 μm), the magnetic products (M2, M3) represent 5 wt% of the source concrete mass, meaning that, taking into account the 74% purity of the M2 magnetic fraction, about 19% of the hydrated cement fraction originally contained in SC was successfully retrieved. The more contaminated fractions, 125–250 μm and 500–1000 μm , yielded 13 and 6% of the hydrated cement in the initial concrete mass, respectively (from 53 to 55% of purity in the M2 magnetic fraction, Fig. 6). Therefore, considering that SC initially contained about 19.3% of hydrated cement, only about 40% of the total cement fraction could be recovered by magnetic separation in the form of high-purity products M2 and M3. This relatively low yield was greatly affected by the low liberation level attained in the 500–1000 μm range and the material loss in the fine residue below 125 μm .

Fig. 8 summarises the distribution of the cement content per each size fraction, showing that the implemented comminution process was able to concentrate the cement content within the size range fractions that can be more effectively subjected to magnetic separation, namely between 125 and 500 μm . However, despite the lower cement content, the amount of waste material in the 500–1000 μm fraction was significant (38% of SC mass). In the future, the liberation of fractions above 500 μm may be improved by an additional grinding step which was out of the scope of this work. The cement fraction not recovered in this range corresponded to as much as 19% of the total cement fraction in SC concrete. The maximum efficiency was attained in the range 250–500 μm , in which about 50% of the total hydrated cement was recovered in

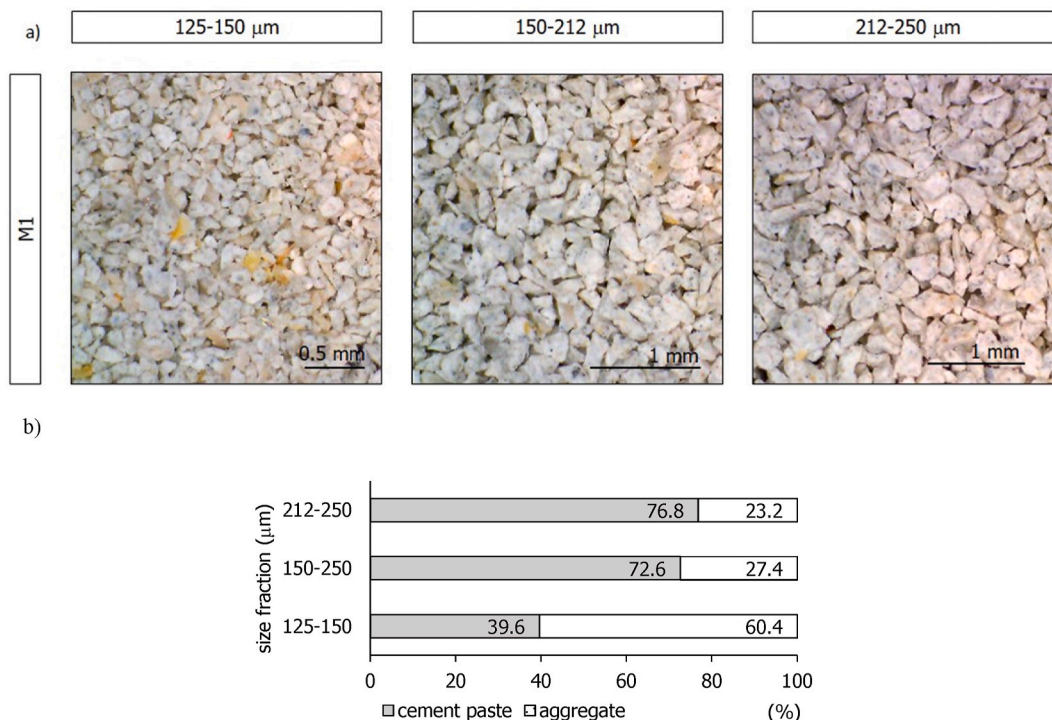


Fig. 7. Magnetic (M1) subdivided fractions (125–150, 150–212 and 212–250 μm) (a) and corresponding cement and aggregate content (b).

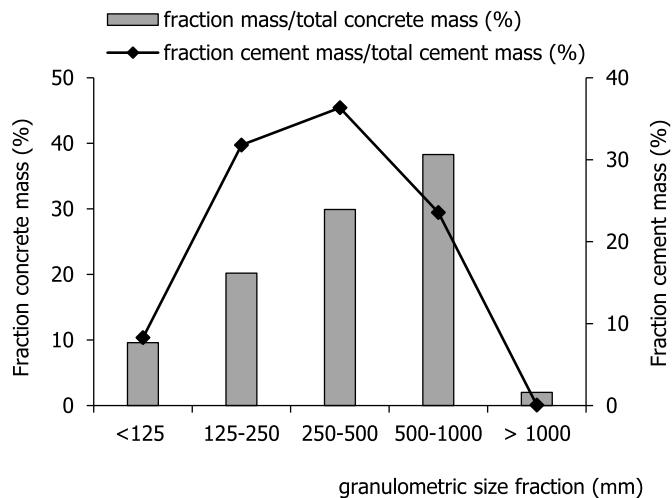


Fig. 8. Concrete and respective cement mass content in each fraction relative to the initial mass of concrete and cement waste, respectively, before magnetic separation.

the form of waste cement with nearly 75% purity.

As discussed in section 2.1, the particles below 125 μm cannot be effectively separated by the magnetic methods, as other attracting forces such as air convection and particle adhesion to the conveyor belt and to adjoining particles can disrupt the procedure. This fraction represented nearly 10 wt% of the initial concrete mass and, according to PTG results, contained about 18 wt% of cement. This means that the original cement fraction that was lost under 125 μm was about 9 wt%. Alternatively, wet magnetic separation techniques are reported to separate particles as small as 75 μm (Svoboda, 2004). Nevertheless, the lost fraction below 125 μm can be used as filler in the production of new concrete.

The level of liberation was further analysed by the Mozley table method, according to 2.7. For the 125–250 μm , 250–500 μm and 500–1000 μm , the amount of separated material was 11, 3.7 and 2.4 wt %, respectively. Moreover, the purity of these separated products in each

fraction was 93.9, 79.8 and 43.4 wt%, respectively. It is thus confirmed that the particles over 500 μm are not sufficiently liberated and that below this size more than 10% of the material presented over 90% cement purity.

From the results obtained in PTG tests, the chosen product to proceed for thermal activation and production of recycled cement was the M3 of the 250–500 μm fraction because it yielded the maximum content of cement fraction, of nearly 80 wt%.

3.4. XRD analysis and acid attack

The XRD diffractograms of both mixture and M3 magnetically separated material for each size fraction are presented in Fig. 9. Despite the qualitative nature of XRD analysis, diffraction peak comparison can aid in validating the procedure described in this paper.

In hydrated cement paste, the main identifiable XRD peaks are portlandite, ettringite and calcite, which correspond to the most crystalline phases and, therefore, more clearly captured by XRD. The nanocrystalline C–S–H hydration products are seldomly identified due to the overlapping of these low-intensity diffraction peaks by more crystalline phases. Moreover, in concrete, the high-intensity peaks corresponding to the aggregates' mineral phases, namely quartz and calcite, tend to minimise low-intensity peaks corresponding to the hydrated cement phases.

The relative peak score of portlandite to the sum of quartz and calcite ($P/(Q + C)$) and quartz/calcite (Q/C) are indicated in Fig. 9. The considered main peaks of portlandite, quartz and calcite were those at 2θ of 34.1, 26.6 and 29.43°, respectively. Overall, a general decrease of the peaks corresponding to the mineral phases of the aggregates can be observed in the magnetic fractions, confirming the effectiveness of the method in reducing the contamination level. Although most identified calcite is associated with limestone aggregate, a part can also result from the waste cement carbonation during grinding, sieving, drying and storage. This affects the level of portlandite increase in the magnetic fractions.

From Fig. 9, it is also confirmed that the most effective separation occurred in the fraction between 250 and 500 μm . Over and under this

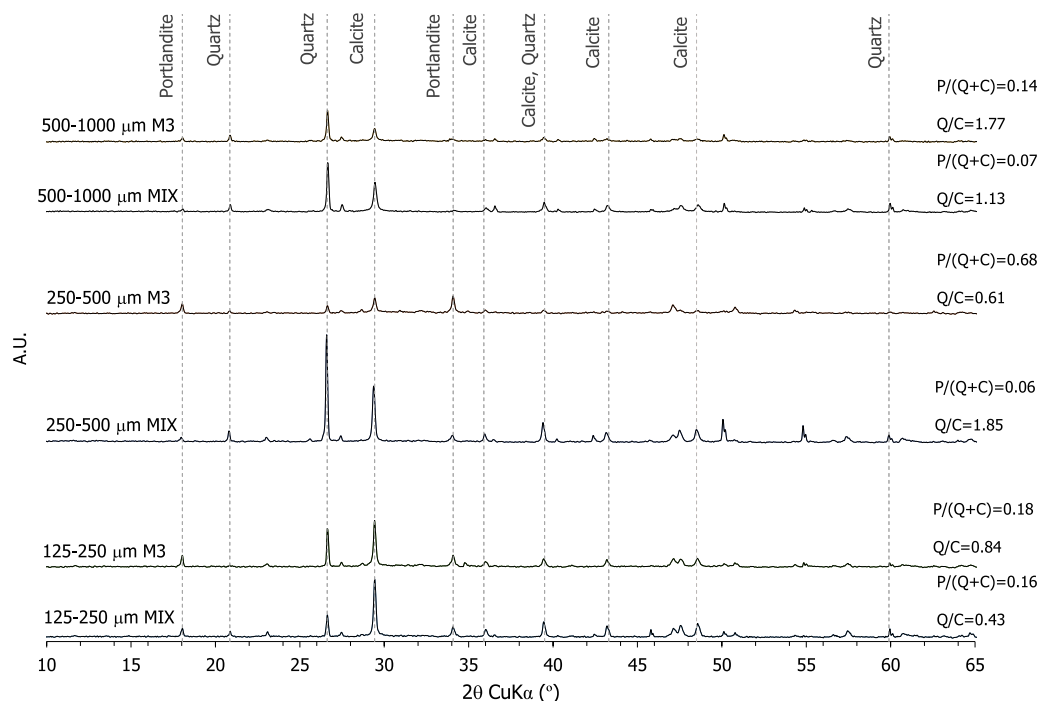


Fig. 9. X-ray diffractogram of mixture and M3 magnetic fraction for each magnetically retrieved size fraction.

range, the relative peak score $P/(Q + C)$ was not as significantly increased as found in the 250–500 μm magnetic fraction (Fig. 9). In particular, the magnetic separation appeared to be poor for particles under 250 μm , in which $P/(Q + C)$ was only slightly increased in the magnetic fraction. Also, the ratio Q/C tended to increase in the magnetic fractions, which may be related to the better liberation of the cement paste from the coarser limestone aggregate than from the fine siliceous sand (with the same average particle size of the analysed fractions). That is, the proportion of sand in the aggregate fraction of the magnetic product is increased. However, as mentioned, calcite from carbonated portlandite in cement paste may contribute to reducing the Q/C ratio in the magnetic fractions. This may explain the inverse trend observed in the highly pure 250–500 μm magnetic fraction.

The acid treatment combined with PTG results allowed the estimation of relative proportioning of concrete constituents in each magnetic fraction. As explained in section 2.5, the hydrochloric acid used in this treatment acts through accelerated leaching of calcium ions, causing the decomposition of cement phases and limestone aggregate. Therefore, the remaining particulate belongs to quartz minerals (from sand) unaffected by this agent. The error between two samples for the acid attack test was below 5%.

Fig. 10 shows each concrete constituent's relative proportion in the mixture and in the final magnetic products (M3), for each size fraction. Compared to the initial mix, the increasing tendency of the relative quartz to calcite ratio (Q/C) in the magnetic fractions is confirmed, as suggested from XRD analysis.

The percentage of siliceous sand in the 250–500 μm size fraction determined by the acid attack was 13.3 wt%. This indicates that the final material comprises 78.8 wt% of cement paste, 13.3 wt% of sand and 7.9 wt% of limestone aggregate. Taking into account an average density of 2640 kg/m^3 and 1320 kg/m^3 (for a hydration degree of 80%, section 3.1) for the aggregates and hydrated cement paste, respectively (section 2.2), the composition in terms of volume percentage corresponds to as much as 88.1% of cement paste and only 11.9% of aggregate.

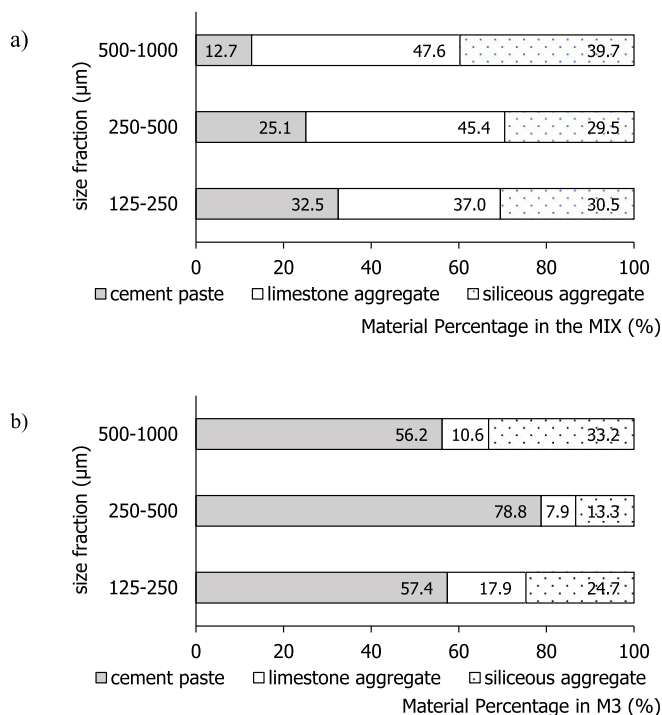


Fig. 10. Relative percentage of cement paste, limestone and siliceous aggregate in (a) the initial mix and in (b) each magnetically retrieved size fraction (M3 products).

In sum, the results obtained through the XRD, PTG and acid attack tests show that the new separation method proposed in this paper provides a way of effectively retrieving cement paste from waste concrete materials.

3.5. Mechanical characterisation of recycled cement pastes

The procedure described in this paper was developed with the purpose of retrieving the cementitious fraction in waste concrete materials to produce an eco-efficient recycled cement. As described in 2.8, the rehydration capacity of this waste cement fraction is recovered through thermal activation. In this study, recycled cement was produced from the less contaminated 250–500 μm magnetic size fraction of waste concrete (M3RC). The 79% cement fraction (see 3.3) in the waste cement reduced to 74% after thermal activation, due to the dehydration and dehydroxylation of hydration products in cement paste, while the aggregates' mass was not significantly affected.

As explained in 2.8, the mechanical strength of a cement paste produced with M3RC was compared against a reference paste with the same water-cement ratio (0.71) produced with recycled cement from source cement paste (RRC). Fig. 11 shows the average compressive and flexural strength of these pastes at 3, 7 and 28 days.

At 28 days, the compressive strength of M3RC paste was 66% of that obtained with reference RRC. This ratio did not vary significantly at 3 and 7 days. Taking into account the cement content of M3RC (74%), the water to binder ratio (w/b) of 0.71 corresponds to a water to cement ratio (w/c) of as high as 0.96, which justifies the mechanical strength reduction. However, the paste with M3RC showed less water demand and higher workability for the same w/b ratio. This means that the higher w/c in M3RC than in RRC pastes can be partly compensated by the reduction of the mixing water for the same workability. The relative flexural strength at 28 days of M3RC compared to RCC paste was slightly higher (76%), since this property varies with the compressive strength according to a power law with an exponent lower than 1 (ACI 318, 2014; CEN, 2004). In other studies of the authors (Bogas et al., 2020a; Real et al., 2020), involving pastes of equal composition (w/b), the compressive strength of RRC paste was similar to higher than that of reference OPC at 3 days and about 30% lower at 28 days.

4. Conclusions

The liberation and separation methods described in this study aimed to obtain individualised hardened concrete constituents, waste cement

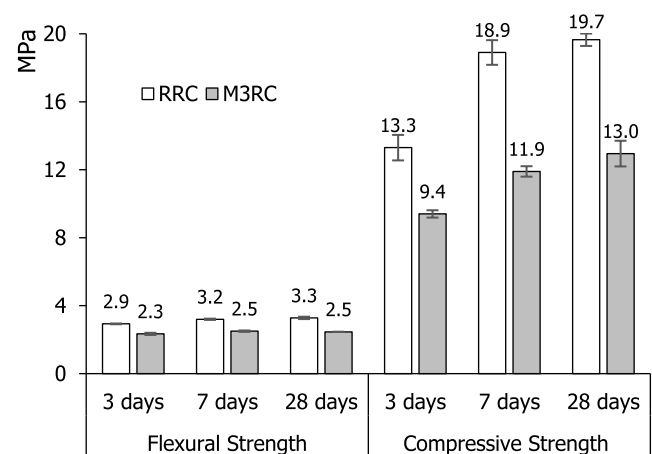


Fig. 11. Flexural and compressive strength at 3, 7 and 28 days of paste with recycled cement from source cement paste (RRC) and with M3 magnetic material from waste concrete (M3RC).

paste and cleaner aggregate, envisioning their re-use as recycled cement and high-quality recycled fine sand, respectively. From the results here obtained, the following conclusions can be drawn:

- At the liberation stage, the comminution circuit adopted in this study effectively concentrated the initial material in the granulometric size fractions suitable for magnetic separation. Around 90 wt% of the original crushed concrete was retained between 125 and 1000 μm , with only about 10 wt% being lost to the finer ($<125 \mu\text{m}$) and coarser ($>1 \text{ mm}$) size ranges.
- The comminution methods were effective in obtaining individualised particles of cement paste and aggregates in the granular mixes, especially in the 125–500 μm size range, as confirmed by qualitative image analysis and the tests performed on the Mozley Table. For particles over 500 μm , liberation was less efficient, but additional crushing steps can be employed to reduce the particle size to the lower fractions and improve the liberation quality.
- Magnetic separation with high-intensity magnets was effective in separating the cement and aggregate particles, especially in the 150–500 μm range. However, the technique is strongly dependent on the liberation quality achieved with the comminution methods. For finer particles (125–150 μm), the magnetic separation was negatively affected by external factors, such as airflow and inability to guarantee a monolayer feeding.
- PTG combined with acid attack demonstrated that it was possible to obtain a magnetic product with a reasonable amount of cement fraction; 57, 79 and 52 wt% for the 125–250 μm , 250–500 μm and 500–1000 μm size fractions, respectively. In the 250–500 μm range, even considering a lower magnetic product (M2), it was possible to retrieve 50 wt% of the total hydrated cement in the form of waste cement with about 75% purity. In terms of volume percentage, the amount of cement paste achieved in this fraction was as much as nearly 90%.
- In total, about 40 wt% of the hydrated cement was retrieved from waste concrete. This moderate yield is expected to be thoroughly improved when the present methodology is scaled up to a demonstration phase, using high performance mechanical crushing equipment and industrial magnetic rollers.

- The non-magnetic product (NM) of all size fractions (125–1000 μm) contained a reduced amount of cement paste (3–11 wt%), proving the method proposed in this study was efficient in obtaining a clean fine aggregate with minor contamination of adhered cement paste.
- Mechanical strength results of pastes produced with recycled cement obtained from waste concrete confirmed the rehydration capacity of this new more eco-efficient binder. The mechanical strength was about 70% of that obtained in pastes with non-contaminated reference recycled cement of equal w/b, which was in agreement with the effective cement content in the M3 magnetic fraction determined by PTG.

CRediT authorship contribution statement

Ana Carriço: Conceptualization, Methodology, Formal analysis, Investigation, Resources, Data curation, Writing – original draft, Writing – review & editing. **José Alexandre Bogas:** Conceptualization, Methodology, Formal analysis, Investigation, Resources, Data curation, Writing – original draft, Writing – review & editing, Funding acquisition, Conceptualization, Methodology, Formal analysis, Investigation, Resources, Data curation, Writing – original draft, Writing – review & editing. **Sofia Real:** Writing – review & editing. **Manuel Francisco Costa Pereira:** Methodology, Funding acquisition.

Declaration of competing interest

The authors declare that they have no known competing financial interests or personal relationships that could have appeared to influence the work reported in this paper.

Acknowledgements

The authors wish to thank the Portuguese Foundation for Science and Technology (FCT) for funding this research under project PTDC/ECI-COM-28308/2017 and unit projects UIDB/ECI/04625/2020 (CERIS) and UID/CTM/04540/2019 (CeFEMA), as well as SECIL for supplying the materials for the experimental campaign. The first author also wishes to thank the financial support of FCT through scholarship SFRH/BD/146033/2019.

Appendices.

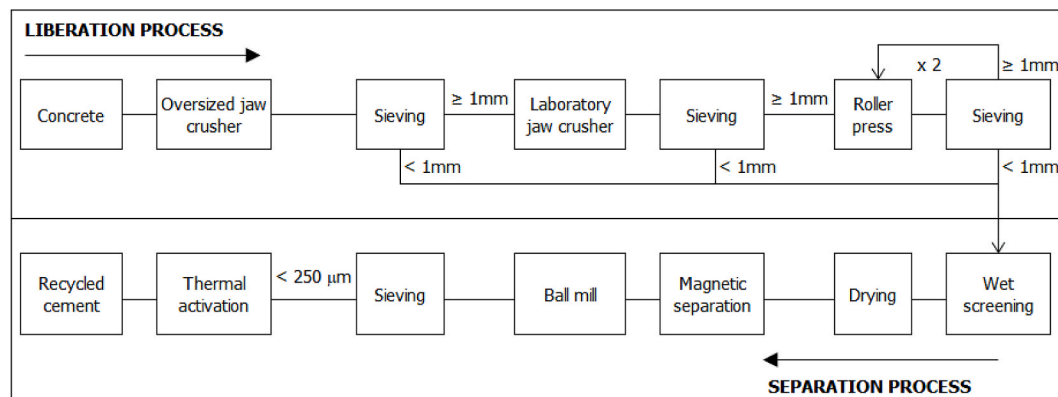


Fig. A.1. Flowchart of the novel liberation and separation method.

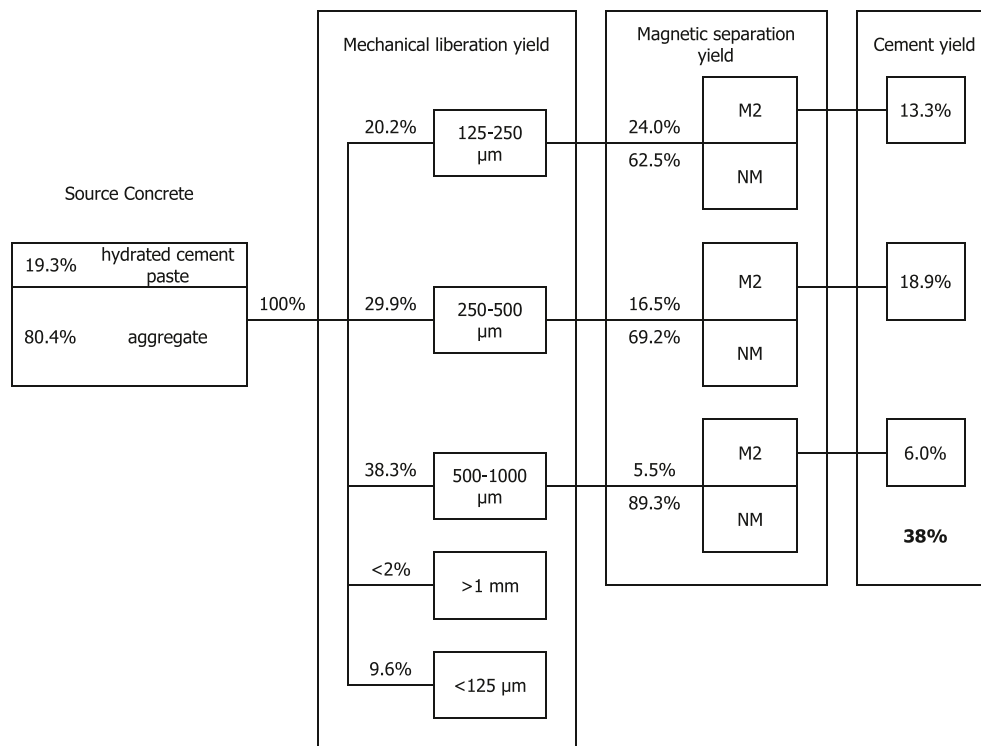


Fig. A.2. Scheme representing the yield obtained at each stage of the novel liberation and magnetic separation procedure (by mass percentage). Only the magnetic product after two scans (M2) is considered in this scheme.

References

- ACI 318, 2014. Building Code Requirements for Structural Concrete. American Concrete Institute.
- Akbarnezhad, A., Ong, K.C.G., 2013. Separation Processes to Improve the Quality of Recycled Concrete Aggregates (RCA), Handbook of Recycled Concrete and Demolition Waste. Woodhead Publishing Limited. <https://doi.org/10.1533/9780857096906.2.246>.
- Al-Bayati, H.K.A., Das, P.K., Tighe, S.L., Baaj, H., 2016. Evaluation of various treatment methods for enhancing the physical and morphological properties of coarse recycled concrete aggregate. *Construct. Build. Mater.* 112, 284–298. <https://doi.org/10.1016/j.conbuildmat.2016.02.176>.
- Angulo, S.C., Ulsen, C., John, V.M., Kahn, H., Cincotto, M.A., 2009. Chemical-mineralogical characterisation of C&D waste recycled aggregates from São Paulo, Brazil. *Waste Manag.* 29, 721–730. <https://doi.org/10.1016/j.wasman.2008.07.009>.
- Bogas, J.A., Carriço, A., Pereira, M.F.C., 2019. Mechanical characterisation of thermal activated low-carbon recycled cement mortars. *J. Clean. Prod.* 218, 377–389. <https://doi.org/10.1016/j.jclepro.2019.01.325>.
- Bogas, J.A., Carriço, A., Tenza-Abril, A.J., 2020a. Microstructure of thermoactivated recycled cement pastes. *Cement Concr. Res.* 138, 106226 <https://doi.org/10.1016/j.cemconres.2020.106226>.
- Bogas, J.A., Pereira, M., Guedes, M., Carriço, A., Hu, S., Sousa, R., 2020b. Separation process of waste hardened concrete for obtaining recycled cement from waste concrete. International patent application PCT/PT2021/050005 priority date 23/02/2021.
- Bru, K., Touzé, S., Bourgeois, F., Lippiatt, N., Ménard, Y., 2014. Assessment of a microwave-assisted recycling process for the recovery of high-quality aggregates from concrete waste. *Int. J. Miner. Process.* 126, 90–98. <https://doi.org/10.1016/j.minpro.2013.11.009>.
- Carriço, A., Bogas, J.A., Guedes, M., 2020a. Thermoactivated cementitious materials - a review. *Construct. Build. Mater.* 250, 118873 <https://doi.org/10.1016/j.conbuildmat.2020.118873>.
- Carriço, A., Real, S., Bogas, J.A., Pereira, M.F.C., 2020b. Mortars with thermo activated recycled cement: fresh and mechanical characterisation. *Construct. Build. Mater.* 256 <https://doi.org/10.1016/j.conbuildmat.2020.119502>.
- CEN, 2019. EN 1015-11 Methods of Test for Mortar for Masonry - Part 11: Determination of Flexural and Compressive Strength of Hardened Mortar. European Committee for Standardization (CEN), Brussels, Belgium.
- CEN, 2016. EN 196-3 Methods of Testing Cement - Part 3: Determination of Setting Times and Soundness. European Committee for Standardization (CEN), Brussels, Belgium.
- CEN, 2004. Eurocode 2: design of concrete structures. <https://doi.org/10.3403/30096437>.
- Chen, W., Jin, R., Xu, Y., Wanatowski, D., Li, B., Yan, L., Pan, Z., Yang, Y., 2019. Adopting recycled aggregates as sustainable construction materials: a review of the scientific literature. *Construct. Build. Mater.* 218, 483–496. <https://doi.org/10.1016/j.conbuildmat.2019.05.130>.
- Collier, N.C., 2016. Transition and decomposition temperatures of cement phases - a collection of thermal analysis data. *Ceram. - Silikaty* 60, 338–343. <https://doi.org/10.13168/cs.2016.0050>.
- Deloitte, 2017. Resource Efficient Use of Mixed Wastes, Improving Management of Construction and Demolition Waste – Final Report. Prepared for the European Commission, DG ENV.
- European Union, 2018. Directive 2018/851 amending directive 2008/98/EC on waste Framework. Off. J. Eur. Union L-150, 109–140.
- European Union, 2011. Commission Decision of 18 November 2011 establishing rules and calculation methods for verifying compliance with the targets set in Article 11 (2) of Directive 2008/98/EC of the European Parliament and of the Council. Off. J. Eur. Union 310, 11.
- Eurostat, 2020. Generation of Waste by Waste Category, Hazardousness and NACE Rev. 2, 12.15.20. activity [WWW Document]. URL: <https://appsso.eurostat.ec.europa.eu/nui/submitViewTableAction.do>.
- Gopalakrishnan, R., Barathan, S., Govindarajan, D., 2012. Magnetic susceptibility measurements on fly ash admixtured cement hydrated with groundwater and seawater. *Am. J. Mater. Sci.* 2, 32–36. <https://doi.org/10.5923/j.materials.20120201.06>.
- Hansen, T., 1992. Recycling of Demolished Concrete and Masonry. Taylor and Francis, London.
- He, Z., Zhu, X., Wang, J., Mu, M., Wang, Y., 2019. Comparison of CO2 emissions from OPC and recycled cement production. *Construct. Build. Mater.* 211, 965–973. <https://doi.org/10.1016/j.conbuildmat.2019.03.289>.
- Katz, A., 2004. Treatments for the improvement of recycled aggregate. *J. Mater. Civ. Eng.* 16, 597–603. [https://doi.org/10.1061/\(asce\)0899-1561\(2004\)16:6\(597\)](https://doi.org/10.1061/(asce)0899-1561(2004)16:6(597)).
- Kirthika, S.K., Singh, S.K., Chourasia, A., 2020. Alternative fine aggregates in production of sustainable concrete- A review. *J. Clean. Prod.* 268, 122089 <https://doi.org/10.1016/j.jclepro.2020.122089>.
- Krour, H., Trauchessec, R., Lecomte, A., Diliberto, C., Barnes-Davin, L., Bolze, B., Delhay, A., 2020. Incorporation rate of recycled aggregates in cement raw meals. *Construct. Build. Mater.* 248, 118217 <https://doi.org/10.1016/j.conbuildmat.2020.118217>.
- Letelier, V., Tarela, E., Muñoz, P., Moriconi, G., 2017. Combined effects of recycled hydrated cement and recycled aggregates on the mechanical properties of concrete. *Construct. Build. Mater.* 132, 365–375. <https://doi.org/10.1016/j.conbuildmat.2016.12.010>.
- Lotfi, S., Deja, J., Rem, P., Mróz, R., Van Roekel, E., Van Der Stelt, H., 2014. Mechanical recycling of EOL concrete into high-grade aggregates. *Resour. Conserv. Recycl.* 87, 117–125. <https://doi.org/10.1016/j.resconrec.2014.03.010>.

- Mistri, A., Bhattacharyya, S.K., Dharmi, N., Mukherjee, A., Barai, S.V., 2020. A review on different treatment methods for enhancing the properties of recycled aggregates for sustainable construction materials. *Construct. Build. Mater.* 233 <https://doi.org/10.1016/j.conbuildmat.2019.117894>.
- Mulder, E., de Jong, T.P.R., Feenstra, L., 2007. Closed Cycle Construction: an integrated process for the separation and re-use of C&D waste. *Waste Manag.* 27, 1408–1415. <https://doi.org/10.1016/j.wasman.2007.03.013>.
- Niry, R.R., Beaucour, A.L., Hebert, R., Noumowé, A., Ledéser, B., Bodet, R., 2013. Thermal stability of different siliceous and calcareous aggregates subjected to high temperature. *MATEC Web Conf* 6. <https://doi.org/10.1051/mateconf/20130607001>.
- Real, S., Carriço, A., Bogas, J.A., Guedes, M., 2020. Influence of the treatment temperature on the microstructure and hydration behavior of thermoactivated recycled cement. *Materials* 13. <https://doi.org/10.3390/ma13183937>.
- Rosenblum, S., Brownfield, I.K., 2000. *Magnetic Susceptibilities of Minerals*. US Department of the Interior, US Geological Survey.
- Shi, C., Li, Y., Zhang, J., Li, W., Chong, L., Xie, Z., 2016. Performance enhancement of recycled concrete aggregate - a review. *J. Clean. Prod.* 112, 466–472. <https://doi.org/10.1016/j.jclepro.2015.08.057>.
- Shigeishi, M., 2017. Separation and collection of coarse aggregate from waste concrete by electric pulsed power. *AIP Conf. Proc.* 1887, 020077. <https://doi.org/10.1063/1.5003560>.
- Silva, R.V., de Brito, J., Dhir, R.K., 2017. Availability and processing of recycled aggregates within the construction and demolition supply chain: a review. *J. Clean. Prod.* 143, 598–614. <https://doi.org/10.1016/j.jclepro.2016.12.070>.
- Sui, Y., Mueller, A., 2012. Development of thermo-mechanical treatment for recycling of used concrete. *Mater. Struct. Constr.* 45, 1487–1495. <https://doi.org/10.1617/s11527-012-9852-z>.
- Svoboda, J., 2004. *Magnetic Techniques for the Treatment of Materials*. Kluwer Academic Publishers. <https://doi.org/10.1007/1-4020-2107-0>.
- Tahar, Z.E.A., Kadri, E.H., Ngo, T.T., Bouvet, A., Kaci, A., 2016. Influence of recycled sand and gravel on the rheological and mechanical characteristic of concrete. *J. Adhes. Sci. Technol.* 30, 392–411. <https://doi.org/10.1080/01694243.2015.1101185>.
- Tam, V.W.Y., Tam, C.M., Le, K.N., 2007. Removal of cement mortar remains from recycled aggregate using pre-soaking approaches. *Resour. Conserv. Recycl.* 50, 82–101. <https://doi.org/10.1016/j.resconrec.2006.05.012>.
- UEPG, 2020. *Annual Review 2019 - 2020*. European Aggregates Association, Brussels, Belgium.
- UNEP, 2019. *Sand and Sustainability: Finding New Solutions for Environmental Governance of Global Sand Resources*. GRID-Geneva. United Nations Environment Programme, Geneva, Switzerland.
- Wang, J., Mu, M., Liu, Y., 2018. Recycled cement. *Construct. Build. Mater.* 190, 1124–1132. <https://doi.org/10.1016/j.conbuildmat.2018.09.181>.